Performance of Er^{3+}-doped chalcogenide glass MOF amplifier applied for 1.53 μm band*

ZHENG Yuan-hui (郑渊慧), **ZHOU Ya-xun** (周亚训)**, **YU Xing-yan** (於杏燕), **QI Ya-wei** (齐亚伟), **PENG Sheng-xi** (彭胜喜), **WU Li-bo** (吴立波), **and YANG Feng-jing** (杨风景)

College of Information Science and Engineering, Ningbo University, Ningbo 315211, China

(Received 1 March 2014)

A model of Er^{3+}-doped chalcogenide glass ($Ga_5Ge_{20}Sb_{10}S_{65}$) microstructured optical fiber (MOF) amplifier under the excitation of 980 nm is presented to demonstrate the feasibility of it applied for 1.53 μm band optical communications. By solving the Er^{3+} population rate equations and light power propagation equations, the amplifying performance of 1.53 μm band signals for Er^{3+}-doped chalcogenide glass MOF amplifier is investigated theoretically. The results show that the Er^{3+}-doped chalcogenide glass MOF exhibits a high signal gain and broad gain spectrum, and its maximum gain for small-signal input (-40 dBm) exceeds 22 dB on the 300 cm MOF under the excitation of 200 mW pump power. Moreover, the relations of 1.53 μm signal gain with fiber length, input signal power and pump power are analyzed. The results indicate that the Er^{3+}-doped $Ga_5Ge_{20}Sb_{10}S_{65}$ MOF is a promising gain medium which can be applied to broadband amplifiers operating in the third communication window.

Document code: A **Article ID:** 1673-1905(2014)03-0184-4

DOI 10.1007/s11801-014-4030-x

Over the past few decades, the rare-earth doped fiber amplifiers have been used in the wavelength division multiplexing (WDM) optical communication systems[1-3]. Various trivalent rare-earth ions, such as Er^{3+}[4], Tm^{3+}[5], Pr^{3+}[6] and Yb^{3+}[7] ions, can be used as the doped active ions of fiber amplifiers operating in different wavelength ranges. In particular, the Er^{3+}-doped fiber amplifier (EDFA) operating in the C-band region, i.e., the third optical communication window (~1.53 μm), is nowadays widely applied in long-haul communications to compensate for the optical loss. After the extensive spreading of EDFAs based on the conventional silica glass, many other novel glass hosts have been developed in order to improve the amplifying performance. Among them, chalcogenide glasses based on chalcogenide elements, such as S, Se and Te, with the addition of other elements, such as Ga, Ge and Sb, have induced a particular interest as glass hosts for rare-earth doped optical devices[8-11], owing to their many interesting properties, such as large absorption and emission sections of the doped rare-earth ions, high host refractive index, low multi-phonon relaxation probability and allowing the increased radiative transition efficiency among rare-earth energy levels. They also possess large rare-earth doped concentration without suffering from the ion-clustering effects. Moreover, because of their transparency from the end of the visible region to the medium infrared region, chalcogenide glasses are very useful in active applications, such as fiber amplifiers and infrared lasers.

In order to further improve the optical signal gain of EDFA, it is crucial to launch much more pump light into the doped fiber, which in turn requires the doped fiber to have a large mode area. However, a very large effective mode area is difficult to obtain in conventional structured single-mode fibers[12]. Therefore, the microstructured optical fiber (MOF)[13-16] is a feasible and attractive solution.

In this paper, a novel Er^{3+}-doped $Ga_5Ge_{20}Sb_{10}Sb_{65}$ chalcogenide microstructured optical fiber amplifier pumped at 980 nm is designed to reveal the amplifying performance at about 1.53 μm.

The transversal section of the designed chalcogenide glass MOF is shown in Fig.1. The transverse structure has three rings of air holes arranged in a triangular lattice. The mode field characteristic of MOF is mainly determined by the geometrical parameters of the hole-to-hole distance (or hole pitch) Λ and the air hole diameter d.

The fundamental mode field distribution of the designed $Ga_5Ge_{20}Sb_{10}Sb_{65}$ glass MOF can be calculated with a finite element method (FEM) by applying a suitable perfect matched layer (PML) condition[17]. The calculated result at the wavelength of 1.53 μm with MOF diameter of D=125 μm, a hole-to-hole distance of Λ=8

* This work has been supported by the National Natural Science Foundation of China (No.61177087), the Graduate Innovative Scientific Research Project of Zhejiang Province (No.YK2010048), the Scientific Research Foundation of Graduate School of Ningbo University (No.G13035), and K. C. Wong Magna Fund and Hu Lan Outstanding Doctoral Fund in Ningbo University.

** E-mail:zhouyaxun@nbu.edu.cn

μm and hole diameter of d=3.2 μm is exhibited in Fig.2. It shows that the chalcogenide glass MOF exhibits a broader mode field distribution compared with the conventional single-mode fiber, indicating that it is a good candidate for infrared amplifier and laser applications in a wide wavelength range.

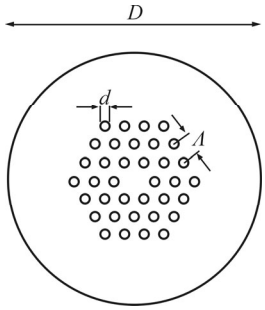

Fig.1 Transversal section of the designed Er^{3+}-doped chalcogenide glass MOF

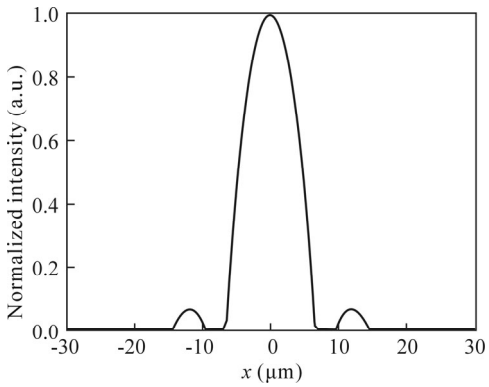

Fig.2 Transverse distribution of the fundamental mode field

The rare-earth Er^{3+} level system in the chalcogenide glasses is quite complex because many processes are involved[18]. The most important Er^{3+} transitions related to the 1.53 μm signal amplification among the energy levels under the excitation of 980 nm pump source are shown in Fig.3. First, the ions at the ground-state level $^4I_{15/2}$ are excited to the excited-state level $^4I_{11/2}$ via the process of ground state absorption (GSA). Then, the ions at the excited-state level $^4I_{11/2}$ decay rapidly to the meta-stable level $^4I_{13/2}$, leading to the population inversion between the $^4I_{13/2}$ and $^4I_{15/2}$ levels. The power enhancement of the transmission signal, via the $^4I_{13/2}\rightarrow{}^4I_{15/2}$ transition, occurs close to the wavelength of 1.53 μm, where the peak of emission spectrum takes place. Other physical phenomena taken into account in the model are the interactions of Er^{3+} pairs: the cross-relaxation of Er^{3+}:$^4I_{9/2}$+Er^{3+}:$^4I_{15/2}\rightarrow Er^{3+}$:$^4I_{13/2}$ +Er^{3+}:$^4I_{13/2}$, in which an ion at the $^4I_{9/2}$ level transfers part of its energy to an ion at the $^4I_{15/2}$ level, both moving to the intermediate $^4I_{13/2}$ level, and the cooperative up-conversion of Er^{3+}:$^4I_{13/2}$+ Er^{3+}:$^4I_{13/2}\rightarrow Er^{3+}$:$^4I_{9/2}$ +Er^{3+}:$^4I_{15/2}$, in which two Er^{3+} ions at the $^4I_{13/2}$ level exchange energy between each other, and then one ion transits to the higher level $^4I_{9/2}$ while the other to the $^4I_{15/2}$ level. For sake of simplicity, the pump excited state absorption (ESA) of ions at the level $^4I_{11/2}$ is neglected.

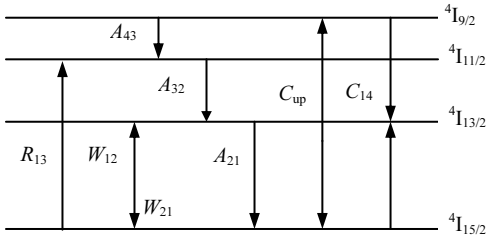

Fig.3 Energy level transitions of Er^{3+} pumped at 980 nm

Under the 980 nm excitation, the level diagram shown in Fig.3 leads to the following rate equations:

$$\frac{\partial N_1}{\partial t} = -W_{12}N_1 - R_{13}N_1 + A_{21}N_2 + W_{21}N_2 + C_{up}N_2^2 - C_{14}N_1N_4,$$

$$\frac{\partial N_2}{\partial t} = W_{12}N_1 - A_{21}N_2 - W_{21}N_2 + A_{32}N_3 - 2C_{up}N_2^2 + 2C_{14}N_1N_4,$$

$$\frac{\partial N_3}{\partial t} = R_{13}N_1 - A_{32}N_3 + A_{43}N_4,$$

$$\frac{\partial N_4}{\partial t} = C_{up}N_2^2 - C_{14}N_1N_4 - A_{43}N_4,$$

$$N_1 + N_2 + N_3 + N_4 = N_T, \quad (1)$$

in which N_1, N_2, N_3 and N_4 represent the populations of the energy levels $^4I_{15/2}$, $^4I_{13/2}$, $^4I_{11/2}$ and $^4I_{9/2}$, respectively, and N_T is the Er^{3+}-doped concentration in the core glass. A_{21}, A_{32} and A_{43} are the spontaneous radiative transition rates from the $^4I_{13/2}$ to $^4I_{15/2}$, $^4I_{11/2}$ to $^4I_{13/2}$ and $^4I_{9/2}$ to $^4I_{11/2}$ levels, respectively. C_{up} is the upconversion energy transfer coefficient and C_{14} is the cross-relaxation energy transfer coefficient. $W_{12/21}$ are the stimulated absorption and emission transition rates at the 1.53 μm band, R_{13} is the stimulated absorption transition rate at the 980 nm pump wavelength, and they can be defined as:

$$W_{12/21} = \frac{\sigma_{a/e}(\upsilon_s)}{h\upsilon_s}P_s(\upsilon_s)E(x,y,\upsilon_s),$$

$$R_{13} = \frac{\sigma_a(\upsilon_p)}{h\upsilon_p}P_p(\upsilon_p)E(x,y,\upsilon_p), \quad (2)$$

where $E(x,y,\upsilon)$ is the transversal mode field profile at frequency υ, P_s and P_p are the signal power and pump power, and σ_a and σ_e are the stimulated absorption and emission cross sections, respectively.

The power propagations of the signal, pump and amplified spontaneous emission (ASE) along the chalcogenide glass MOF are described by the following differential equations:

$$\frac{dP_s}{dz} = [\sigma_e(\upsilon_s)n_2(\upsilon_s) - \sigma_a(\upsilon_s)n_1(\upsilon_s)]P_s(\upsilon_s) - \alpha(\upsilon_s)P_s(\upsilon_s),$$

$$\frac{dP_p}{dz} = -\sigma_a(\upsilon_p)n_1(\upsilon_p)P_p(\upsilon_p) - \alpha(\upsilon_p)P_p(\upsilon_p),$$
$$\frac{dP_{ASE\pm}}{dz} = \pm[\sigma_e(\upsilon)n_2(\upsilon) - \sigma_a(\upsilon)n_1(\upsilon)]P_{ASE\pm}(\upsilon) \pm 2h\upsilon\sigma_e(\upsilon)n_2(\upsilon)m\alpha(\upsilon)P_{ASE\pm} \quad , \tag{3}$$

where α is the MOF background loss, n_i (i=1, 2) is the overlap integral of the normalized signal mode intensity $E(x,y,\upsilon)$ and the population N_i of the energy level:

$$n_i(\upsilon) = \iint_S N_i(x,y,z)\left|E(x,y,\upsilon)\right|^2 dxdy \quad , \tag{4}$$

where S is the surface of the MOF doped region.

The above set of differential equations is nonlinear due to the ion-ion interaction, and it should be numerically integrated via an iterative procedure based on the fourth-order Runge-Kutta algorithm with appropriate boundary conditions:

$$P_p(0) = P_{p0}, \quad P_s(0) = P_{s0},$$
$$P_{ASE+}(0) = P_{ASE-}(L) = 0 \quad , \tag{5}$$

where L is the active fiber length, and P_{s0} and P_{p0} are the input signal power and pump power, respectively.

The relevant spectroscopic parameters, together with optical losses, refractive index and the doped concentration of Er^{3+}, used for numerical calculations are listed in Tab.1. The stimulated absorption and emission cross sections of Er^{3+} in the 1500—1620 nm region shown in Fig.4 are determined from the measured absorption spectra of $Ga_5Ge_{20}Sb_{10}Sb_{65}$ chalcogenide glass using the Beer-Lambert law and the McCumber theory[19], respectively. The $Ga_5Ge_{20}Sb_{10}Sb_{65}$ chalcogenide glass is fabricated with the high-temperature melting and annealing method.

Tab.1 Parameters used for numerical calculations[8,18]

Parameter	Symbol	Value	Unit
Spontaneous radiative transition rate	A_{21}	250	s^{-1}
	A_{32}	775	s^{-1}
	A_{43}	18868	s^{-1}
Cooperative upconversion coefficient	C_{up}	3.0×10^{-23}	m^3s^{-1}
Cross-relaxation coefficient	C_{14}	5.0×10^{-24}	cm^2
Emission cross section at 980 nm	σ_e	3.84×10^{-21}	cm^2
Absorption cross section at 980 nm	σ_a	4.78×10^{-21}	cm^2
Background loss for signal light	α	2.0	dB/m
Background loss for pump light	α	3.0	dB/m
Refractive index	n	2.25	---
Er^{3+} doped concentration	N_T	5.76×10^{18}	cm^{-3}

Fig.5 displays the signal gain spectrum simulated by single-wavelength operation for an Er^{3+}-doped $Ga_5Ge_{20}Sb_{10}Sb_{65}$ chalcogenide glass MOF amplifier pumped at 980 nm. The MOF amplifier with 300 cm fiber length is forward pumped with a pump power of 200 mW. The input signal wavelength is scanned from 1500 nm to 1620 nm and the signal power is fixed at -40 dBm. As can be observed, the gain spectrum exhibits a broadband profile even in the extended C-band region to 1500 nm, which can be employed in multi-channel amplifying applications. Under this pumping scheme and operating condition, the maximum small signal gain exceeds 20 dB and the signal gain at 1538 nm is about 22.3 dB.

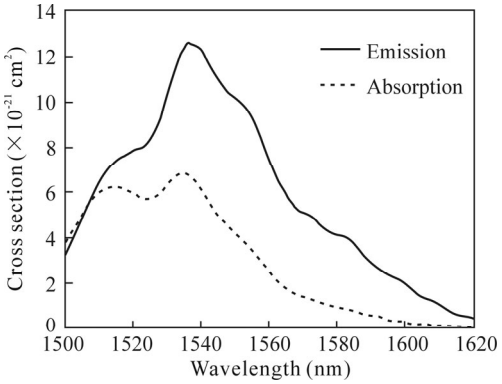

Fig.4 Stimulated absorption and emission cross sections of Er^{3+} in chalcogenide glass

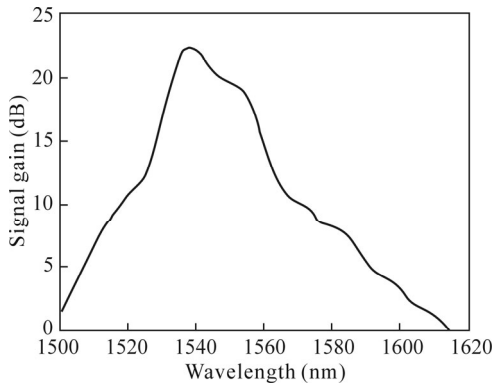

Fig.5 1.53 μm-band gain spectrum of the Er^{3+}-doped chalcogenide glass MOF

Fig.6 presents the effect of fiber length on the signal gain at 1538 nm pumped at 980 nm. The pump power and signal power are kept at 200 mW and -40 dBm, respectively. As can be seen, the signal gain increases near-linearly with the fiber length at the beginning. With the further increase of fiber length, the signal gain saturates gradually and begins to decay after reaching the maximum value. The optimal fiber length is about 600 cm under the current operating parameters.

Fig.7 gives the variation of the 1538 nm signal gain with pump power under the fiber length of 300 cm and input power of -40 dBm. It is shown that the threshold pump power is about 42 mW, and after this value, the signal gain increases rapidly with pump power and then gradually up to about 25 dB.

Fig.8 gives the variation of the 1538 nm signal gain with input power under the fiber length of 300 cm and pump power of 200 mW. It is shown that the signal gain

is almost constant under the small signal input condition. However, with the increase of input power, the signal gain decreases gradually due to the gain saturation effect.

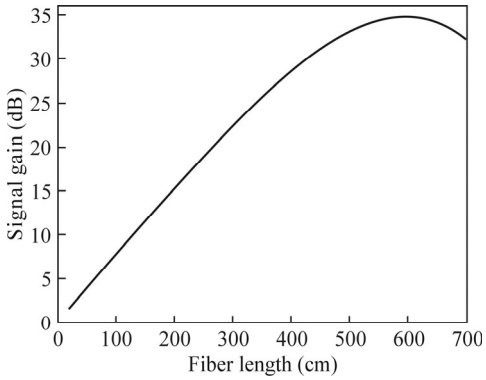

Fig.6 Variation of signal gain with the fiber length at 1538 nm pumped at 980 nm

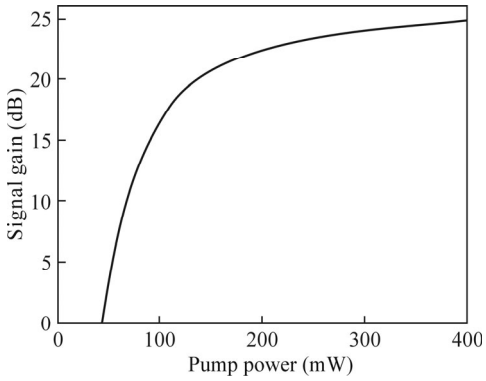

Fig.7 Variation of signal gain at 1538 nm with pump power under the fiber length of 300 cm and input power of -40 dBm

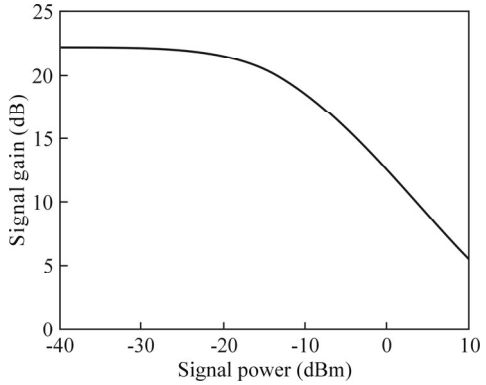

Fig.8 Variation of the 1538 nm signal gain with input power under the fiber length of 300 cm and pump power of 200 mW

The 1.53 μm band amplifying performance of Er^{3+}-doped chalcogenide glass ($Ga_5Ge_{20}Sb_{10}Sb_{65}$) MOF amplifier pumped at 980 nm has been investigated theoretically. It is shown that it can provide broad signal gain spectrum in the third communication window. Under the excitation of 200 mW pump power, the maximum signal gain exceeds 22 dB with the 300 cm MOF length in the small signal operation. The results indicate that the Er^{3+}-doped $Ga_5Ge_{20}Sb_{10}Sb_{65}$ chalcogenide glass MOF amplifier can become a promising candidate applied in the 1.53 μm band optical communication systems.

References

[1] S. Singh, A. Singh and R. S. Kaler, Optik- International Journal for Light and Electron Optics **124**, 95 (2013).

[2] M. M. Ismail, M. A. Othman, Z. Zakaria, M. H. Misran, M. A. Meor Said, H. A. Sulaiman, M. N. Shah Zainudin and M. A. Mutalib, Procedia Engineering **53**, 294 (2013).

[3] H. Y. Hsu, Y. L. Yu, S. K. Liaw, R. Y. Liu and C. S. Shin, Optics & Laser Technology **56**, 307 (2014).

[4] M. Michalska, J. Swiderski and M. Mamajek, Optics & Laser Technology **60**, 8 (2014).

[5] A. H. M. Husein and F. I. El-Nahal, Optik- International Journal for Light and Electron Optics **124**, 4052 (2013).

[6] A. H. M. Husein and F. I. El-Nahal, Optics Communications **283**, 409 (2010).

[7] T. Wei, Z. Y. Tan, J. F. Li and J. H Zhu, Optik- International Journal for Light and Electron Optics **124**, 2459 (2013).

[8] M. De Sario, L. Mescia, F. Prudenzano, F. Smektala, F. Deseveday, V. Nazabal, J. Troles and L. Brilland, Optica & Laser Technology **41**, 99 (2009).

[9] F. Prudenzano, L. Mescia, L. Allegretti, M. De Sario, F. Smektala, V. Moizan, V. Nazabal, J. Troles, J. L. Doualan, G. Canat, J. l. Adam and B. Boulard, Optical Materials **31**, 1292 (2009).

[10] F. Prudenzano, L. Mescia, L. A. Allegretti, M. De Sario, T. Palmisano, F. Smektala, V. Moizan, V. Nazabal and J. Troles, Journal of Non-Crystalline Solids **355**, 1145 (2009).

[11] C. S. Yi, P. Q. Zhang, S. X. Dai, X. S. Wang, Y. H. Wu, T. F. Xu and Q. H. Nie, Optics Communications **311**, 270 (2013).

[12] L. Brilland, F. Smektala, G. Renversez, T. Charter, J. Troles, T. Nguyen, N. Traynor and A. Monteville, Optics Express **14**, 1280 (2006).

[13] B. L. Behera, A. Maity, S. K. Varshney and R. Datta, Optics Communications **307**, 9 (2013).

[14] T. L. Cheng, K. Asano, Z. C. Duan, T. H. Tuan, W. Q. Gao, D. H. Deng, T. Suzuki and Y. Ohishi, Optics Communications **318**, 105 (2014).

[15] D. J. Xu, H. R. Song, W. Wang, Y. Fan and B. Yang, Optik-International Journal for Light and Electron Optics **124**, 1290 (2013).

[16] V. P. Minckovich, A. V. Kiryanov, A. B. Sosky and L. I. Sotskaya, Journal of the Optical Society of America B **21**, 1161 (2004).

[17] F. Brechet, J. Marcou, D. Pagnoux and P. Roy, Optical Fiber and Technology **6**, 181 (2000).

[18] K. Kadono, T. Yazawa, S. Jiang, J. Porque, B. C. Hwang and N. Peyghambarian, Journal of Non-Crystalline Solids **331**, 79 (2003).

[19] D. E. McCumber, Physical Review **134**, A299 (1964).